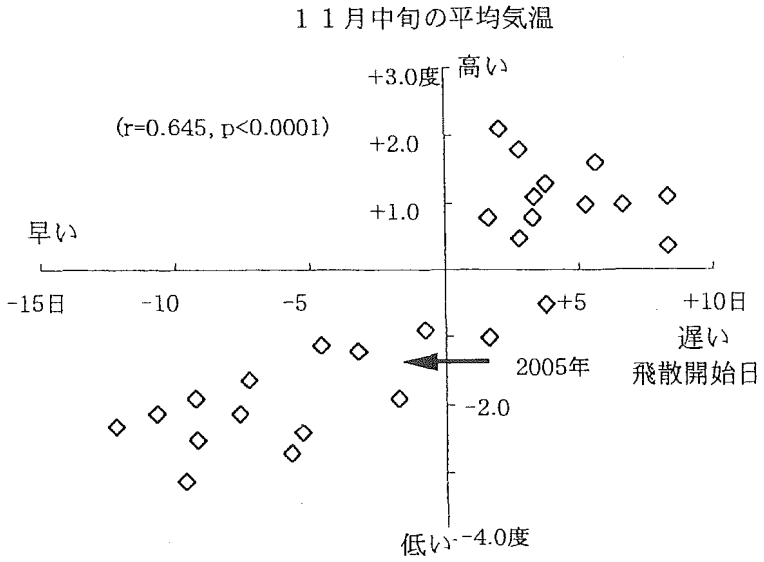

図6　11 月中旬の平均気温とスギ花粉飛散開始日

結論

フィールド調査をもとに2006年のスギ花粉飛散総数は，津市で2,500前後個/cm^{2}と予想した。気象情報および早期スギ花粉飛散からも予想数は妥当と考えられる。平年値やや弱と予想した。2005年の花粉飛散結果はスギが過去3番目，ヒノキ科が過去最高の大量飛散であった。

三重大学医学部耳鼻咽喉科スギ花粉情報

http://www.medic.mie-u.ac.jp/kafun

携帯電話用ページ

http://www.medic.mie-u.ac.jp/kafun/i,

http://www.medic.mie-u.ac.jp/kafun/ez

3)　スギ花粉における秋の気象条件と花粉飛散の影響

佐々木康二[1)]，湯田厚司[2)]，三品朋子[1)]，鈴木あゆ美[1)]，間島雄一[2)]

[1)]三重大学医学部医学科，[2)]三重大学大学院医学系研究科耳鼻咽喉頭頸部外科

要　旨

スギ花粉飛散総数は夏の気象が影響し，花粉症は晩冬から春におこる。従って，秋の気象やスギ花粉症は関心が少ない。秋はスギ花粉症に関係ない季節であろうかについて検討した。

［目的］秋のスギ花粉飛散と秋の気象がスギ花粉症に及ぼす影響を検討した。

［方法］2004年秋のスギ花粉飛散を測定し，その時の花粉症状有無と春の症状出現時期を検討した。秋の気象がスギ花粉飛散開始時期に及ぼす影響を検討した。

［結果］2004年秋には過去最高のスギ花粉が計測され，スギ花粉症例には短期間の花粉症状を認める患者が約1/4に認めた。秋に症状のある患者は，春のスギ花粉症の発症が有意に早かった。11月中旬の平均気温は飛散開始に影響し，気温が低いほどスギ花粉は早期に飛散した。

［結論］秋の気象や花粉飛散もスギ花粉症に影響する。

Ⅰ．はじめに

スギ花粉症の治療は，抗原（スギ花粉）回避と薬物治療が基本となる。抗原回避のためには，どの時期にスギ花粉が飛散し，どれくらいの花粉が飛散するかをあらかじめ予想することが重要である。

抗原回避には花粉飛散予想は最も重要である。三重大学耳鼻咽喉科教室では，これまでに夏の気象とスギ雄花着花状況から非常に精度の高い花粉予想をたててきた。2005年のスギ花粉予想は極めて大量飛散と予想していた。ところでスギ花粉の飛散時期は２月から４月とされるが，実は秋にも飛散することが知られている。また，夏のみでなく秋の気象も花粉にとっては重要かもしれない。そこで，秋の花粉と気象に注目し，これまでに見向きもされなかった秋のスギ花粉についての初めての検討を行った。

Ⅱ．方法

1）スギ花粉飛散調査

これまでの春の花粉調査に加えて秋の花粉調査を追加した。方法は，三重大学医学

部臨床研究棟屋上（9階建て）に設置したダーラム型花粉収集器のスライド上に落下するスギ花粉をforbus blackley染色液で染色し，検鏡した。個数は，1平方cm当たりで表す。なおスライドは毎日午後3時に交換した。

2）気象状況と花粉飛散開始時期

気象状況は津地方気象台ホームページから参照した。三重県内4ヵ所（津，四日市，上野，尾鷲）の平均気温をダウンロードし，統計解析に利用した。各地の気象は温暖の差がでるため，地域毎に平均気温を算出し，各年の平均値とその地域の平年値の差で表示する事により是正した。花粉飛散開始時期は，当グループが保持する過去の飛散計測データから求めた。極少量のスギ花粉飛散では症状の出ない花粉症患者も多いため，一日あたり5個/cm^2以上飛散した日を飛散開始時期と考えた。患者症状発現時期を考えた本格飛散開始日を視野にした検討となる。飛散開始時期も地域で異なるため，気象と同じく，各地の平均値を算出し，その差を求めた。例えば，津市ならば，津市の［(2003年秋の平均気温)－(過去の平均気温)］および［(2004年の飛散開始日)－(平均飛散開始日)］を計算することとした。秋の平均気温は月ごと，或いは上・中・下旬ごとなど，様々な期間で検討し，どれが相関性があるかを検討した。

3）アンケート調査

三重大学を含む県下3病院の耳鼻咽喉科に来院したスギ花粉症患者（計149名）を対象とした。患者には来院時にその趣旨を説明し，同意をえられた患者のみに調査した。まず，来院時に秋の花粉症状の有無を聞き取り調査した。同時に2005年のスギ花粉症発症時期を聴取した。

Ⅲ．結果

1）2004年秋の花粉飛散実態

スギ花粉は2月中旬から4月初旬に飛散するとされるが，10月および11月にも少量ではあるがスギ花粉飛散が観測された（図1）。1平方センチあたりのスギ花粉飛散数は少数であったが，総計は50個/cm^2にも及び，スギ花粉症状を来しうる花粉飛散が計測された。津市における秋のスギ花粉飛散総数では過去最高であった。秋のスギ花粉は10月6日に初観測され，かなり早い時期での観測となった。この結果からは，春のスギ花粉症時期でない秋にも花粉症症状が認められる可能性が考えられる。

2）2005年春のスギ花粉飛散実態

2005年2月から4月のスギ花粉飛散結果を図2に示す。2005年は総数11,052個/cm^2

の飛散があり，飛散開始日（1個以上のスギ花粉が連続2日以上飛散する日の最初）は2月23日であった。2005年春のスギ花粉飛散は過去20年間で3番目の大量飛散であり。極めて多い飛散を計測した。秋のスギ花粉が多く飛散すると翌年春のスギ花粉も多く飛散するとされており，2004年秋のスギ花粉飛散数に矛盾しない結果であった。飛散開始日は2月23日であったが，1月11日から2月2日までの間に1個/cm²以下の飛散が計9日観察された。従って，2月上旬までは飛散前ではあるが，少量のスギ花粉を計測した時期となる。この期間に症状のあった場合を飛散前症状とし，2月中旬発症例を除き，2月23日以降で症状出現の場合を花粉飛散後症状とした。

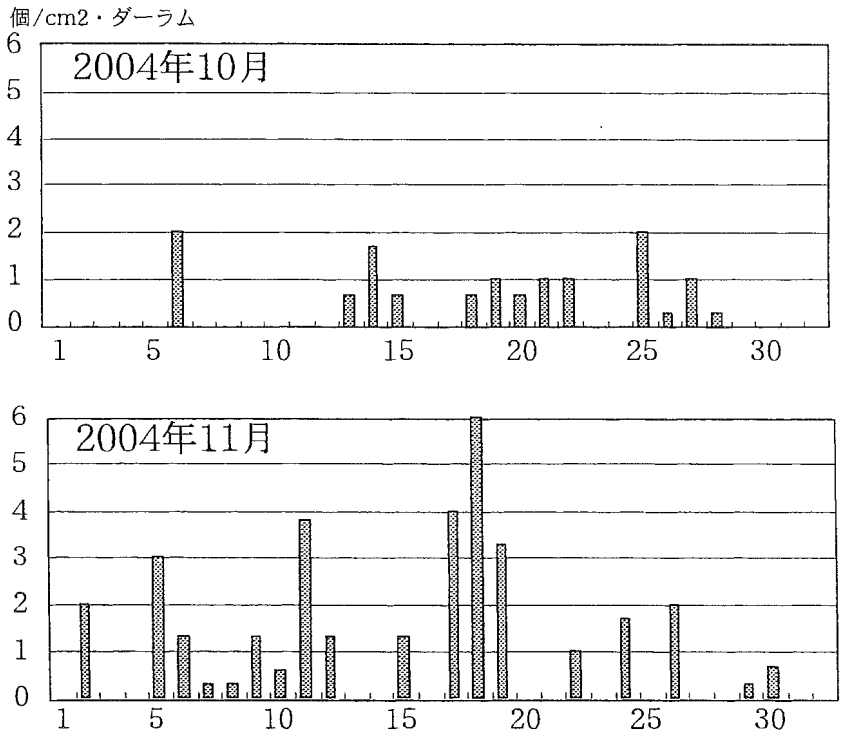

図1　2004年秋のスギ花粉飛散

2004年10月初旬から少量ながらスギ花粉飛散が認められた。飛散個数としては，すべての花粉症患者が発症するほどではないが，長期間にわたって飛散している。（津市三重大学での計測）

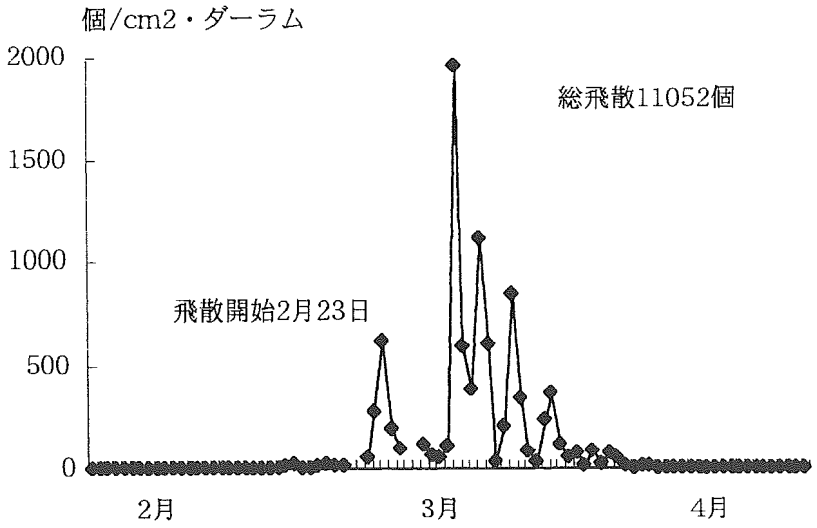

図2　2005年春のスギ花粉飛散

2005年春のスギ花粉飛散は2月23日より飛散開始し，大量の飛散が計測された。これは過去20年間で3番目の飛散数であった。（津市三重大学での計測）

3）秋の花粉症症状

問診による秋の花粉症症状の有無を図3に示した。花粉症の有無については，感冒などとの鑑別が必要であるが，発熱が無いこと，眼症状の出現などから花粉症状との鑑別を患者自身に判断さ

せた。特異的IgE抗体を測っていないため，厳格に秋のスギ以外の花粉症（ブタクサ，ヨモギなど）とは鑑別できていない。秋のスギ花粉飛散の多少にかかわらず，すでに，毎年秋の花粉症がある例は判定不能に含めた。その結果，秋の花粉症状は全体の23.4％に認められた（判断不可能またはわからないが22.4％存在する）。しかし，調査したすべての患者は秋のスギ花粉飛散の認識はなく，何らかの花粉症と認識していた患者はいたものの，スギ花粉症状と認識していた患者はいなかった。

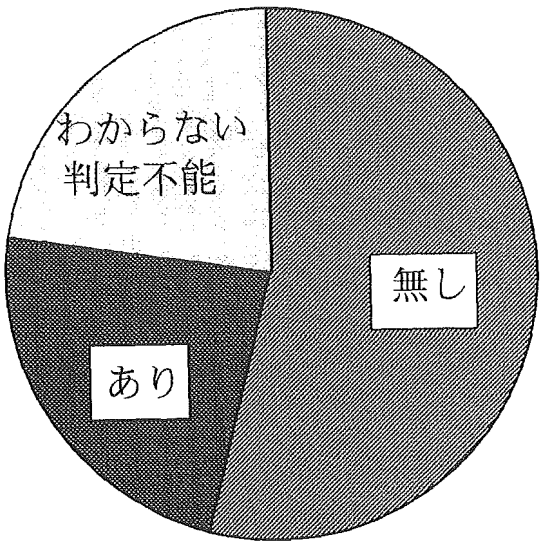

図3　秋のスギ花粉症状の有無
問診により秋のスギ花粉症状を聴取した。

これらの「秋のスギ花粉症状あり」の患者は少量の飛散も反応していることとなる。そこで，秋の花粉症状の有無と，2005年春の花粉症症状の発症日を検討した。表1に示すように秋の花粉症状がある例は，無い例よりも有意に花粉飛散前からの発症が認められた（$p = 0.026$）。

表1　秋のスギ花粉症状と花粉症状発症日
（$p = 0.026$，2乗検定）

	飛散前症状（2月初旬以前）	飛散後症状（2月下旬以前）
秋症状なし	8	42
秋症状あり	9	13

4）秋の気象とスギ花粉飛散開始

スギ花粉は夏の気象に左右され，11月には花序が形成されている。しかし，2月のスギ花粉飛散には休眠打破と呼ばれる寒気の気象条件が必要とされ，開始時期は秋の気象に左右される可能性がある。1994年（気象条件は前年秋）から2005年までの秋の平均気温と花粉飛散開始時期を検討した。平均気温は各月を上中下旬の約10日毎の平均気温とした。花粉飛散開始は，過去の三重大学耳鼻咽喉科教室のスギ花粉飛散計測データを参照した。スギ花粉の飛散は年毎に異なり，3週間前後の差がでることもある。スギ花粉の本格飛散は，ほとんどの患者が発症する1日あたり5個以上の花粉飛散日とした。三重県内4ヵ所でのデータを採用したため，各地区毎に平均気温と花粉飛散開始時期の平均を算出し，平均値との差で検討した。その結果，11月中旬の気象がスギ花粉飛散開始と最も密接に関連し，11月中旬の平均気温が低いほど飛散開始が早かった（$r = 0.645$，$p < 0.0001$）。この結果から，11月中旬の寒気がスギ花粉飛散開始に大きく影響すると考えられる。

Ⅳ．考　　察

スギ花粉症は夏の気象が飛散総数に影響し，晩冬から春の気象がスギ花粉飛散の実際に関与する。従って，秋の気象はあまり重要な要素がないとみられてきた経緯がある。そこで今回，これまであまり見向きもされなかった秋のスギ花粉について検討した。

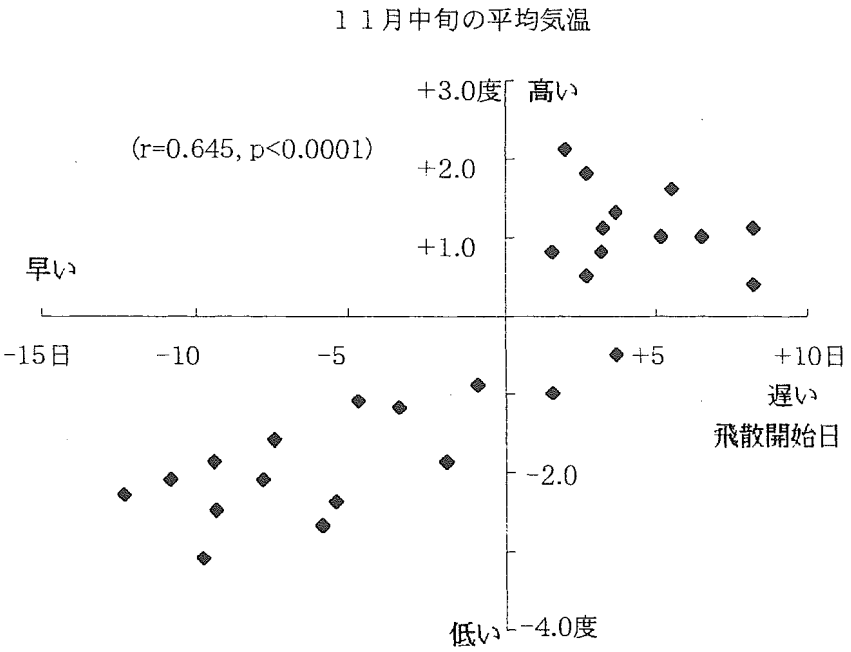

図4　11月中旬の平均気温とスギ花粉飛散開始

11月中旬の気象がスギ花粉飛散開始と最も密接に関連し，11月中旬の平均気温が低いほど飛散開始が早い。

その結果として，非常に重要な見識を得た。秋にも少量ながらスギ花粉が飛散しているが，スギ花粉症症状が出現していると認識している患者はなかった。実際には1/4程度の例で秋のスギ花粉症が発症しており，患者に認識させる必要があると思われた。また，この時期に花粉症症状を持つ患者は，花粉症本番の2月には早期から発症しやすかった。この結果から，秋にスギ花粉症がある例は早期からの投薬を考えるべきであり，逆にスギ花粉症が早くから発症する例では秋にも警戒が必要である。

スギ花粉症の本格飛散は，秋の気象，特に11月中旬の気温が低いと飛散開始が早くなっていた。従って，11月中旬の平均気温により，スギ花粉の飛散開始日が予想できる。これは，スギ花粉治療には極めて重要であり，いつからスギ花粉症の予防または治療が必要かの指標となるであろう。これらの結果を踏まえて患者個々の対応に応用できると考えられる。

Ⅴ．付　　記

筆頭著者佐々木康二，共著者三品朋子，鈴木あゆ美は三重大学医学部に在学する学生である。本研究は三重大学医学部4年生の実習として，耳鼻咽喉・頭頸部外科学教室湯田厚司教官の指導のもとに行った。

厚生労働科学研究費補助金（免疫アレルギー疾患予防・治療研究事業）
研究報告書
リアルタイムモニター飛散数と現状の治療によるQOLの関連性の評価と花粉症根治療法の開発
スギ花粉症に対する免疫療法の奏功機序における制御性T細胞および共抑制分子の関与

分担研究者　岡野光博　岡山大学大学院医歯薬学総合研究科　耳鼻咽喉・頭頸部外科助教授

研究要旨
今回我々は、スギ花粉症に対する免疫療法の奏功機序に制御性T細胞や共抑制分子が関与するのか検討した。標準化スギ花粉エキスを用い免疫療法を行ったスギ花粉症患者（免疫療法群）、および免疫療法非施行の患者（非免疫療法群）を対象とした。スギ花粉飛散期に採血を行いPBMCを分離しCryｊ1にて刺激した。培養細胞上のCD4陽性CD25強陽性細胞比率およびPD-1、B7-H1およびBTLA陽性細胞比率をFACSにて解析した。また培養上清中のIL-5やIL-10などのサイトカインをELISAにて測定した。免疫療法群ではCryｊ1刺激によるCD4陽性CD25強陽性細胞比率が有意に増加した。Cryｊ1刺激によるPD-1陽性細胞比率には両群で差を認めなかったが、免疫療法群ではB7-H1陽性細胞比率が増加する傾向を示し、さらにBTLAは免疫療法群で有意に発現が亢進した。免疫療法群ではIL-5産生が有意に抑制されたが、IL-10産生に関しては免疫療法群、非免疫療法群ともに有意な産生を認めなかった。これらの結果より、スギ花粉症に対する免疫療法の奏功機序に制御性T細胞および共抑制分子BTLAがIL-10非依存性に関与する可能性が示唆された。

A研究目的
花粉症の根治をめざすには、花粉アレルゲンに対する免疫寛容を誘導する必要がある。免疫寛容には、①不応答（unresponsiveness/anergy：アナジー）、②除去(deletion)、③免疫偏向・抑制（immune deviation/suppression)の３つのメカニズムが知られている。なかでも制御性T細胞が免疫偏向・抑制を介して免疫療法の奏功機序に関与する可能性が、いくつかのアレルギー疾患で報告されている。また免疫寛容の誘導メカニズムのひとつに共抑制分子の働きが注目されている。今回我々は、スギ花粉症に対する免疫療法の奏功機序に制御性T細胞や共抑制分子が関与するのか検討した。

B方法
１．対象
標準化スギ花粉エキスを用い免疫療法を行ったスギ花粉症患者（免疫療法群：n=11)、および免疫療法非施行の患者（非免疫療法群：n=10）を対象とした。スギ花粉飛散期に採血を行い、末梢血単核細胞（PBMC）を分離した。
２．Cryｊ1刺激によるCD4陽性CD25強陽性細胞の誘導
PBMCをCryｊ1にて刺激し、培養7日目の細胞を回収し、CD4陽性CD25強陽性細胞の比率をFACSにて解析し、無刺激の場合と比較した。
３．Cryｊ1刺激による共抑制分子の誘導
今回は共抑制分子として PD-1、B7-H1 およびBTLAを検討した。PBMCをCryｊ1にて刺激し、培養7日目の細胞を回収し、共抑制分子陽性細胞の比率をFACSにて解析し、無刺激の場合と比較した。
４．Cryｊ1刺激によるサイトカイン産生
PBMCをCryｊ1にて刺激し、培養3日目の上清を回収し、上清中のIL-5、IL-10およびTGF-・濃度をELISAにて解析し、無刺激の場合と比較した。

C結果
１．Cryｊ1刺激によるCD4陽性CD25強陽性細胞の誘導
免疫療法群では、無刺激と比較してCryｊ1刺激によりCD4陽性CD25強陽性細胞が3.86%増加した。一方非免疫療法群では1.91%の増加に留まり、両群の間に有意差（p=0.041)を認めた。
２．Cryｊ1刺激による共抑制分子の誘導
Cryｊ1刺激によるPD-1発現の変化は、免疫療法群（+0.60%）と非免疫療法群（+0.65%）との間で差を認めなかった（p=0.805)。またCryｊ1刺激によるB7-H1発現の変化は、免疫療法群(+0.47%)と非免疫療法群（+0.09%）との間で傾向差を認めた（p=0.067)。さらにCryｊ1刺激によるBTLAの発現は非免疫療法群で2.24%低下した。一方、免疫療法群ではBTLAの発現はCryｊ1刺激により0.97%増加し、非免疫療法群と比較して有意な（p<0.001）発現増加を認めた。
３．Cryｊ1刺激によるサイトカイン産生の変化
非免疫療法群ではCryｊ1刺激により300pg/ml

のIL-5産生が誘導された。一方、免疫療法群では45pg/ml と有意な産生抑制がみられた (p=0.007)。IL-10 および TGF-・に関しては両群とも有意な産生を認めなかった。

D 考察

イネ科花粉症などでは免疫療法により制御性 T 細胞が誘導されることが報告されている。今後より詳細なマーカーの検討などが必要であるが、一般的に制御性T細胞はCD25強陽性であることから、今回の結果はスギ花粉症においても制御性 T 細胞が免疫療法の奏功機序に関与する可能性を示唆している。制御性 T 細胞の作用機序として、IL-10 や TGF-・などの制御性サイトカインの分泌を介する作用と、cell-cell contact を介する作用が知られている。今回の検討では IL-10 および TGF-・の明らかな産生がみられなかったことから、誘導された制御性 T 細胞は IL-10 非依存性に cell-cell contact などを介して奏功機序に関与する可能性が示唆された。

今回検討した共抑制分子の中では、免疫療法群においてCry j 1 刺激によるBTLA の有意な発現増加がみられた。BTLA は自己免疫疾患などの Th1 応答においてアナジーを誘導し免疫制御に関与することが報告されている。今回の検討では Th2 型の免疫疾患においても本共抑制分子が免疫寛容に関与する可能性を示唆している。

E 結論

スギ花粉症に対する免疫療法を行うことにより制御性T細胞および共抑制分子BTLAの発現が誘導されることが明らかとなった。今後はこれらの細胞および分子が機能的にアレルゲンに対する免疫寛容を誘導するのか検討を進める必要がある。

F 健康危険情報

なし

G 研究発表

1. 論文発表

1) Okano M, Hattori H, et al. Nasal exposure to Staphylococcal enterotoxin enhances the development of allergic rhinitis in mice. Clinical and Experimental Allergy 35: 506-514, 2005.
2) Maeda M, Okano M, et al. Glycofrom analysis of Japanese cedar pollen allergen, Cry j 1. Bioscience Biotechnology Biochemistry 69: 1700-1705, 2005.
3) Hattori H, Okano M, et al. Signals through CD40 play a critical role in the pathophysiology of Schistosoma mansoni egg antigen-induced allergic rhinitis in mice. American Journal of Rhinology (in press).
4) Okano M, Fujiwara T, et al. Presence and characterization of PGD2-related molecules in nasal mucosa of patients with allergic rhinitis. American Journal of Rhinology (in press).
5) Sugimoto H, Okano M, et al. CRTH2-specific binding characteristics of ^{3}H-ramatroban and its effects on PGD_2-, 15-deoxy-^{12,14}-PGJ2- and indomethacin-induced agonist responses. British Journal of Pharmacology (in press).
6) Okano M, Sugata Y, et al. EP2/EP4-mediated suppression of antigen-specific human T cell responses by prostaglandin E2. Immunology (in press).

2. 学会発表

1) 岡野光博: アレルギー疾患における免疫療法の位置づけ. 第 17 回日本アレルギー学会春季臨床大会 (教育講演 7). 2005. 6.
2) 岡野光博:アレルギー性鼻炎の免疫病態と治療. 第 55 回日本アレルギー学会秋季学術大会 (教育講演 4)、2005. 10.
3) 岡野光博:鼻過敏症のマネジメント. 日本アレルギー協会東北支部学術講演会. 2005. 11.

知的財産権の出願・登録状況

1. 特許取得

なし

2. 実用新案登録

なし

3. その他

なし

Biosci. Biotechnol. Biochem., **69** (9), 1700–1705, 2005

Glycoform Analysis of Japanese Cedar Pollen Allergen, Cry j 1*

Megumi MAEDA,[1] Maiko KAMAMOTO,[2] Katsuhiko HINO,[3] Shigeto YAMAMOTO,[3] Mariko KIMURA,[4] Mitsuhiro OKANO,[5] and Yoshinobu KIMURA[1,2,†]

[1]*Division of Biomolecular Science, Graduate School of Natural Science and Technology, Okayama University, Okayama 700-8530, Japan*
[2]*Department of Bioresources Chemistry, Faculty of Agriculture, Okayama University, Okayama 700-8530, Japan*
[3]*Fujisaki Institute, Hayashibara Biochemical Laboratory, Inc., Fujisaki, Okayama 702-8006, Japan*
[4]*Faculty of Food Culture, Department of Food Systems, Kurashiki Sakuyo University, Nagao-Tamashima, Kurashiki 710-0292, Japan*
[5]*Department of Otolaryngology-Head and Neck Surgery, Okayama University Graduate School of Medicine and Dentistry, Okayama 700-8558, Japan*

Received April 1, 2005; Accepted May 25, 2005

In our previous study (Y. Kimura *et al.*, *Biosci. Biotechnol. Biochem.*, 69, 137–144 (2005)), we found that plant complex type *N*-glycans harboring Lewis a epitope are linked to the mountain cedar pollen allergen Jun a 1. Jun a 1 is a glycoprotein highly homologous with Japanese cedar pollen glycoallergen, Cry j 1. Although it has been found that some plant complex type *N*-glycans are linked to Cry j 1, the occurrence of Lewis a epitope in the *N*-glycan moiety has not been proved yet. Hence, we reinvestigated the glycoform of the pollen allergen to find whether the Lewis a epitope(s) occur in the *N*-glycan moiety of Cry j 1. From the cedar pollen glycoallergen, the *N*-glycans were liberated by hydrazinolysis and the resulting sugar chains were *N*-acetylated and then coupled with 2-aminopyridine. Three pyridylaminated sugar chains were purified by reversed-phase HPLC and size-fractionation HPLC. The structures were analyzed by a combination of exo- and endo-glycosidase digestions, sugar chain mapping, and electrospray ionization mass spectrometry (ESI-MS). Structural analysis clearly indicated that Lewis a epitope (Galβ1-3(Fucα1-4)GlcNAcβ1-), instead of the Galβ1-4(Fucα1-6)GlcNAc, occurs in the *N*-glycans of Cry j 1.

Key words: *N*-glycan; Lewis a epitope; pollen allergen; Japanese cedar pollen; Cry j 1

In our previous study,[1)] we found that Lewis a epitope (Galβ1-3(Fucα1-4)GlcNAcβ-) occurs in the *N*-glycan moiety of mountain cedar pollen allergen, Jun a 1. Such plant complex type *N*-glycans bearing Lewis a epitope in addition to a combination of β1-2 xylosyl and α1-3 fucosyl residues have been found among several plant glycoproteins.[2–5)] In the case of the Japanese cedar pollen allergen Cry j 1, although some structures of *N*-glycans linked to this glycoallergen have been proposed,[6,7)] the Lewis a epitope has not been found in the *N*-glycan moiety. Midoro-Horiuti *et al.* have cloned a cDNA of Jun a 1 and found that Jun a 1 possesses a high level of amino acid sequence homology with Cry j 1.[8)] This finding suggests that the *N*-glycan moiety of Jun a 1 might be homologous with that of Cry j 1. Hence, we started a reinvestigation of glycoform of Cry j 1 to confirm the occurrence of the Lewis a epitope. Structural analysis clearly indicated that the Lewis a epitope does occur in the *N*-glycan moiety of Cry j 1, showing that the *N*-glycan moiety of Cry j 1 is also homologous with that of Jun a 1.

Materials and Methods

Materials. Cry j 1 was purified from Japanese cedar pollen as described in previous papers.[6,9)] An Asahipak NH2P-50 column (0.46 × 25 cm) was purchased from Showa Denko (Tokyo, Japan), and a Cosmosil 5C18-AR

* This work was supported in part by grants from the Ministry of Education, Science, Sports, and Culture of Japan (Basic Research (C), No. 17580300 for Y.K).

† To whom correspondence should be addressed. Fax: +81-86-251-8388; E-mail: yosh8mar@cc.okayama-u.ac.jp

Abbreviations: PA-, pyridylamino; RP-HPLC, reverse-phase HPLC; SF-HPLC, size-fractionation HPLC; ESI-MS, electrospray ionization mass spectrometry; Hex, hexose; HexNAc, *N*-acetylhexosamine; Deoxhex, deoxyhexose; Pen, pentose; MFX, Xylβ1-2Manβ1-4GlcNAcβ1-4(Fucα1-3)GlcNAc-PA; M3FX, Manα1-6(Manα1-3)(Xylβ1-2)Manβ1-4GlcNAcβ1-4(Fucα1-3)GlcNAc-PA; GN1M3FX, GlcNAcβ1-2Manα1-6(Manα1-3)(Xylβ1-2)Manβ1-4GlcNAcβ1-4(Fucα1-3)GlcNAc-PA; GN2M3FX, GlcNAcβ1-2Manα1-6(GlcNAcβ1-2Manα1-3)(Xylβ1-2)Manβ1-4GlcNAcβ1-4(Fucα1-3)GlcNAc-PA; GFGN2M3FX, $Gal_1Fuc_1GlcNAc_2Man_3Xyl_1Fuc_1GlcNAc_2$-PA; G2F2GN2M3FX, $Gal_2Fuc_2GlcNAc_2Man_3Xyl_1Fuc_1GlcNAc_2$-PA

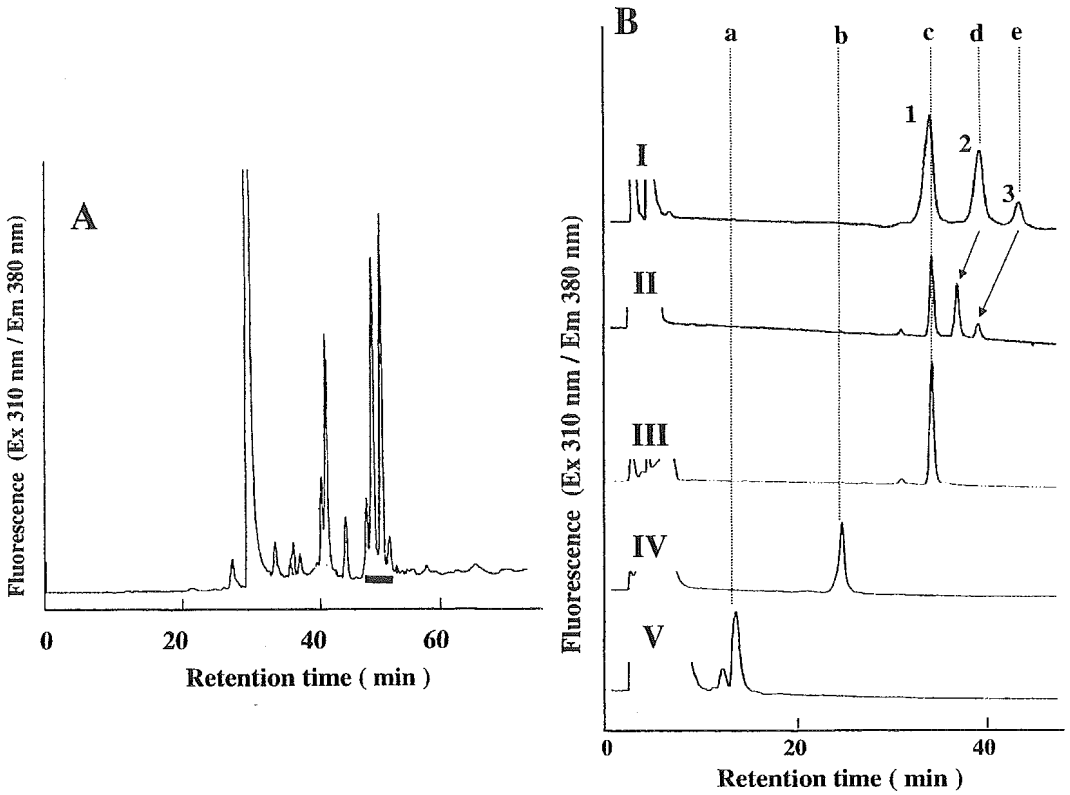

Fig. 1. HPLC Profiles of PA-Sugar Chains from Cry j 1 and Exoglycosidase Digests.

A, RP-HPLC of PA-sugar chains from Cry j 1. The PA-sugar chains were pooled as indicated by the horizontal bars. B, SF-HPLC of PA-sugar chains pooled in A. I, PA-sugar chains obtained in A; II, α1-3/4 specific fucosidase digest of I; III, β1-3/6 specific galactosidase digest; IV, the diplococcal β-*N*-acetylglucosaminidase digest of III; V, jack bean α-mannosidase of IV. Dotted lines (a, b, c, d, and e) indicate the elution positions of authentic PA-sugar chains: a, MFX; b, M3FX; c, GN2M3FX; d, GFGN2M3FX; e, G2F2GN2M3FX.

column (0.6 × 25 cm) from Nacalai Tesque (Kyoto). GN2M3FX and M3FX were prepared from the glycoproteins of oil palm pollens and ricin D.[10,11] GN1M3FX was prepared from glycoproteins of oil palm pollens[10] and *Ginkgo biloba* pollens.[12] α-Mannosidase (jack bean) and β1-3/6 specific β-galactosidase (recombinant expressed in *E. coli*) were purchased from Sigma (St. Louis, MO). β-*N*-acetylglucosaminidase (*Diplococcus pneumonia*) was purchased from Boehringer (Mannheim, Germany). α1-3/4 Specific α-fucosidase (*Streptomyces* sp. 142) and Lacto-*N*-biosidase (*Streptomyces* sp. 142) were purchased from Takara (Kyoto, Japan).

Preparation of pyridylaminated N-glycans from Cry j 1. *N*-Glycans were released by hydrazinolysis (100 °C, 12 h, in 200 µl of anhydrous hydrazine) from lyophilized glycoallergens (about 50 mg). After *N*-acetylation of the hydrazinolysate with saturated ammonium bicarbonate (400 µl) and acetic anhydride (20 µl), the acetylated hydrazinolysate was desalted using Dowex 50 × 2 resins. Pyridylamination of the sugar chains was done by the method of Natsuka and Hase.[13] Separation of PA-sugar chains was done by HPLC on a Jasco 880-PU HPLC apparatus with a Jasco 821-FP Intelligent Spectrofluorometer, using the Shodex Asahipak NH2P-50 column (0.46 × 25 cm) and the Cosmosil 5C18-AR column (0.6 × 25 cm). On the Cosmosil 5C18-AR column, the PA-sugar chains were eluted by increasing the acetonitrile concentration in 0.05% TFA linearly from 0 to 10% at a flow rate of 1.2 ml/min. In the case of size-fractionation HPLC using the Asahipak NH2P-50 column, the PA-sugar chains were eluted by increasing the water content in the water-acetonitrile mixture from 36 to 62% linearly in 60 min at a flow rate of 0.7 ml/min.

Electrospray ionization (ESI) mass spectrometry. ESI-MS analysis of PA-sugar chains was done as described in our previous reports,[14] using a Perkin Elmer Sciex API-III triple-quadrupole mass spectrometer with an atmospheric-pressure ionization ion source.

Glycosidase digestion of PA-sugar chains. Digestion with jack bean α-mannosidase, diplococcal β-*N*-acetylglucosaminidase, and Lacto-*N*-biosidase was done using about 200 pmol of the PA-sugar chains under the conditions described in a previous report.[1] Digestion with the α-fucosidase was done using 200 pmol in 25 mM Na-citrate buffer, pH 5.0 for 16 h. The resulting glycosidase-digests were analyzed by SF-HPLC using an Asahipak NH2P-50 column (0.46 × 25 cm).

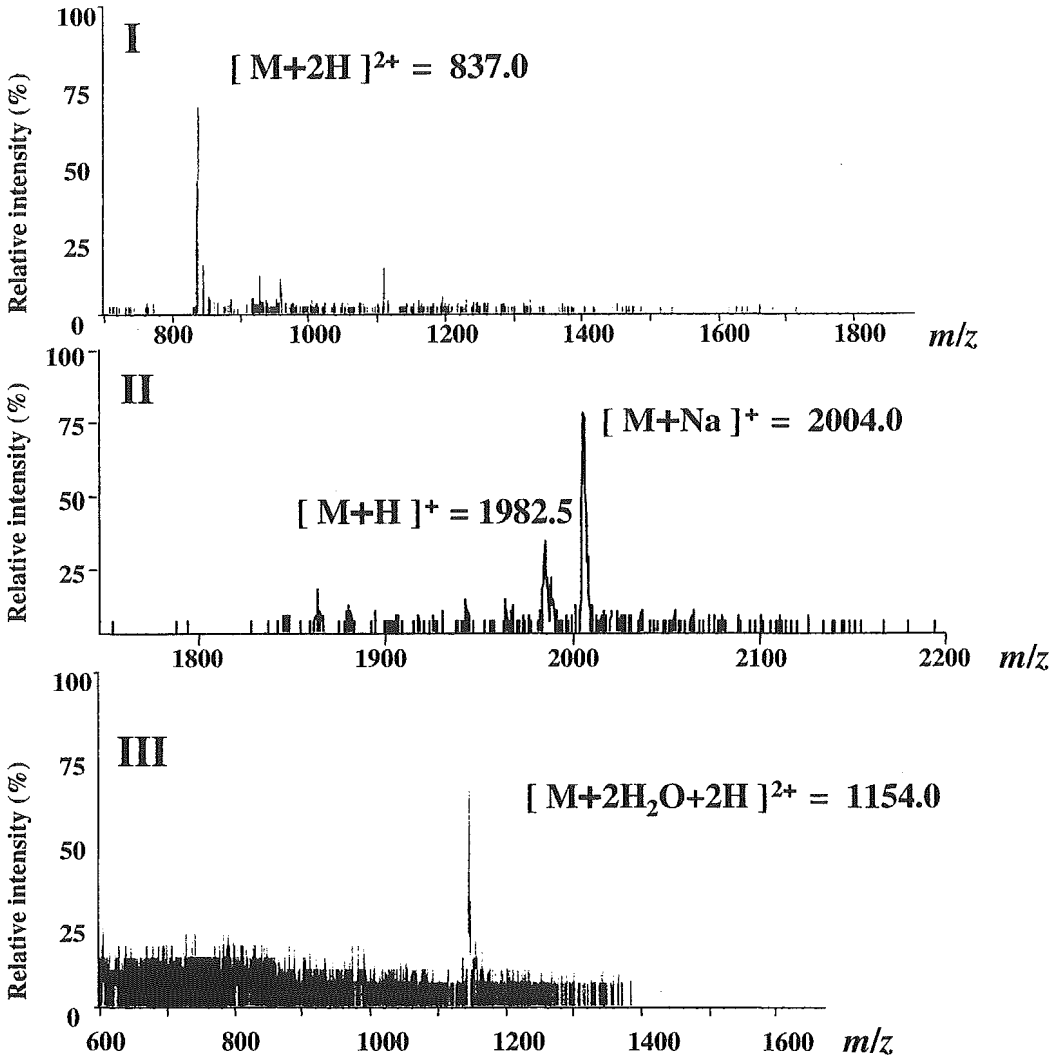

Fig. 2. ESI-MS Spectra of PA-Sugar Chains 1, 2, and 3.
I, PA-sugar chain 1 (GlcNAc2Man3Xyl1Fuc1GlcNAc2-PA); II, PA-sugar chain 2 (Gal1Fuc1GlcNAc2Man3Xyl1Fuc1GlcNAc2-PA); III, PA-sugar chain 3 (Gal2Fuc2GlcNAc2Man3Xyl1Fuc1GlcNAc2-PA).

Results and Discussion

ESI-MS analysis and exoglycosidase digestion of PA-Sugar chains from Cry j 1

First the PA-sugar chains from Cry j 1 were partially purified by RP-HPLC, as shown in Fig. 1A. The PA-sugar chains were pooled as indicated by the horizontal bar. When other peaks observed on the chromatograms were analyzed by SF-HPLC, almost all the peaks were recovered in the run-through fraction. Hence we judged that these peaks were not *N*-glycans. As shown in Fig. 1B, three PA-sugar chains (peak-1, peak-2, and peak-3) from Cry j 1 were separated from the *N*-glycan fraction on the ODS column. The elution position of peak 1 coincided with that of GN2M3FX (from Jun a 1), peak 2 with that of $Gal_1Fuc_1GlcNAc_2Man_3Xyl_1Fuc_1GlcNAc_2$-PA (from Jun a 1), and peak 3 with that of $Gal_2Fuc_2GlcNAc_2Man_3Xyl_1Fuc_1GlcNAc_2$-PA (from Jun a 1) on SF-HPLC, suggesting that the component of *N*-glycan of Cry j 1 is very similar to that of Jun a 1. These results, obtained from this preliminary analysis, agreed well with those of previous reports,[6,7] except for the absence of $Gal_1Fuc_1GlcNAc_2Man_3Xyl_1GlcNAc_2$, found as a minor component in a previous report.[6]

ESI-MS analysis of peak 1 showed a single signal at *m/z* 837.0 $[(M + 2H)^{2+}]$, suggesting that this PA-sugar chain consists of $(HexNAc)_3(Hex)_3(Deoxyhex)_1(Pen)_1$-(HexNAc-PA) or $GlcNAc_2Man_3Xyl_1Fuc_1GlcNAc_2$-PA (Fig. 2I). ESI-MS analysis of peak 2 showed a major signal at *m/z* 2004.0 $[(M + Na)^+]$ (*m/z* 1982.5 $[(M + H)^+]$ as a minor signal), suggesting that this PA-sugar chains consists of $(Hex)_4(HexNAc)_3(Deoxyhex)_2$-$(Pen)_1$(HexNAc-PA) or $Gal_1Fuc_1GlcNAc_2Man_3Xyl_1$-$Fuc_1GlcNAc_2$-PA (Fig. 2II). ESI-MS analysis of peak 3 showed single signal at *m/z* 1154.0 [(M +

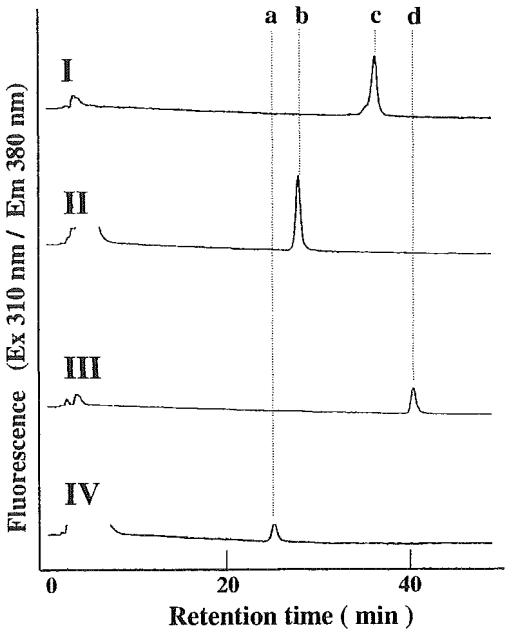

Fig. 3. SF-HPLC of Lacto-*N*-biosidase and α-Fucosidase Digests of PA-Sugar Chains 2 and 3 in Fig. 1B I.

I, PA-sugar chain 2; II, the lacto-*N*-biosidase digest of I; III, PA-sugar chain 2; IV, the lacto-*N*-biosidase digest of III. Dotted lines (a, b, c, and d) indicate the elution positions of authentic PA-sugar chains: a, M3FX; b, GN1M3FX; c, GFGN2M3FX; d, G2F2GN2M3FX.

$2H_2O + 2H)^{2+}$], suggesting that this PA-sugar chain consists of $(Hex)_5(HexNAc)_3(Deoxyhex)_3(Pen)_1$-(HexNAc-PA) or $Gal_2Fuc_2GlcNAc_2Man_3Xyl_1Fuc_1$-$GlcNAc_2$-PA (Fig. 2III). These results obtained by ESI-MS analysis support the deduced structures described above.

When a mixture of three *N*-glycans was treated with α1-3/4 fucosidase, as shown in Fig. 1B II, peak 1 was not digested but peaks 2 and 3 were, suggesting that the fucosyl residues are bound by an α1-3 or α1-4 linkage. When the α1-3/4 fucosidase digest was treated with diplococcal β-galactosidase, galactosyl residue was not released (data not shown). On the contrary, the de-fucosylated PA-sugar chains from peaks 2 and 3 were digested by β1-3/6 specific galactosidase and the elution position of the galactosidase digests converged on that of GN2M3FX (Fig. 1B III). These results indicated that the galactosyl residues were bound to outer GlcNAc residue(s) by a β1-3 or β1-6 linkage. The de-galactosylated product was converted to M3FX by diplococcal β-*N*-acetylglucosaminidase digestion (Fig. 1B IV), suggesting that two GlcNAc residues were bound to the M3FX structure by β1-2 linkage. Finally, the β-*N*-acetylglucosaminidase digest was converted to MFX by jack bean α-mannosidase digestion, as shown in Fig. 1B V.

Endoglycosidase digestion of PA-sugar chains of peaks 2 and 3

To determine the linkage mode of the galactosyl residue, peaks 2 and 3 were treated with mixture of α1-3/4 fucosidase and lacto *N*-biosidase. It has been reported that the latter enzyme can release the Galβ1-3GlcNAc unit but not the Galβ1-4GlcNAc unit from galactose-containing complex type *N*-glycans.[15] As shown in Fig. 3II, the product obtained from peak 2 by the endoglycosidase digestion was eluted at the elution position of GN1M3FX, indicating that one Galβ1-3GlcNAc unit was released. On the other hand, the product obtained from peak 3 by endoglycosidase digestion was eluted at the elution position of M3FX, indicating that two Galβ1-3GlcNAc units were released. These results suggest that peaks 2 and 3 carry a β1-3 galactosy residue(s) and an α1-4 fucosyl residue(s) rather than a β1-4 galactosy residue(s) and an α1-3 fucosyl residue(s), suggesting that the Lewis a epitope(s) harbor in the *N*-glycan moiety of Cry j 1.

Comparison of N-glycan structures between Cry j 1 and Jun a 1

From the results of sugar chain mapping, ESI-MS analysis, and exo- and endo-glycosidase digestion, we found that Lewis a epitope (Galβ1-3 (Fucα1-4)-GlcNAcβ1-), instead of the Galβ1-4 (Fucα1-6)-GlcNAcβ1- unit, does occur in *N*-glycan moiety of Cry j 1. The proposed structures of *N*-glycans are shown in Table 1. Concerning the structure of peak 2, from these results, it is difficult to determine which mannosyl residue (α1-6 arm Man or α1-3 arm Man) harbors the Lewis a epitope. But in previous reports,[6,7] it was reported that the $Gal_1Fuc_1GlcNAc_1$ unit is bound to the α1-6 arm mannosyl residue, and hence the structure of peak 2 might be Galβ1-3 (Fucα1-4)GlcNAcβ1-2Manα1-6(GlcNAcβ1-2Manα1-3)Manβ1-4GlcNAcβ1-4GlcNAc. Comparing the oligosaccharide structures of Cry j 1 and Jun a 1, basically both glycoallergens bear very similar *N*-glycan compositions (the Lewis a epitope-containing type and the typical biantennary plant complex type *N*-glycan ($GlcNAc_2Man_3Xyl_1$-$Fuc_1GlcNAc_2$)). As shown in Table 1, in the case of Cry j 1, Lewis a epitope-containing structures (peaks 2 and 3) account for about 50% of total *N*-glycans. On the other hand, in the case of Jun a 1, such complex type structures account for 25% of total *N*-glycans. This observation suggests that expressions of α1-4 fucosyl and β1-3galactosyl transferases or some trimming glycosidases (β-galactosidase and β-hexosaminidase) working in the vacuole or cell wall might be slightly different in two kinds of pollen (the mountain cedar and the Japanese cedar), since Cry j 1 and Jun a 1 are highly homologous protein.[8]

Although the physiological importance of the Lewis a epitope in the *N*-glycan moiety of Cry j 1 and Jun a 1 remains to be understood, it is reasonable to assume that the glycan moiety might be involved in plant cellular communication in analogy with the Lewis a epitope occurring in animal cells.

Table 1. Comparison of *N*-Glycan Structure between Jun a 1 and Cry j 1

Proposed Structures	Relative amount (%)		
	Jun a 1 (A)[a]	Jun a 1 (B)[a]	Cry j 1
GlcNAcβ1-2 { Manα1-6 / Manα1-3 } Manα1-4GlcNAcβ1-4GlcNAc (2: Xylβ1; 3: Fucα1)	nd	3	nd
GlcNAcβ1-2 Manα1-6 / GlcNAcβ1-2 Manα1-3 Manβ1-4GlcNAcβ1-4GlcNAc (2: Xylβ1; 3: Fucα1)	75	76	47 Peak 1
Fucα1-4 / Galβ1-3 { GlcNAcβ1-2Manα1-6 / GlcNAcβ1-2Manα1-3 } Manβ1-4GlcNAcβ1-4GlcNAc (2: Xylβ1; 3: Fucα1)	23	21	38 Peak 2
Fucα1 (4) Galβ1-3GlcNAcβ1-2Manα1-6 / Galβ1-3GlcNAcβ1-2Manα1-3 (4: Fucα1) Manβ1-4GlcNAcβ1-4GlcNAc (2: Xylβ1; 3: Fucα1)	2	nd	15 Peak 3

[a]Reference 1).
nd, not detected.

Acknowledgments

The authors are grateful to the ESI-MS Laboratory of Okayama University.

References

1) Kimura, Y., Kamamoto, M., Maeda, M., Okano, M., Yokoyama, M., and Kino, K., Occurrence of Lewis a epitope in *N*-glycans of a glycoallergen, Jun a 1, from mountain cedar pollen. *Biosci. Biotechnol. Biochem.*, **69**, 137–144 (2005).
2) Fichette-Lainè, A.-C., Gomord, V., Cabanes, M., Michalski, J.-C., Macary, M. S., Foucher, B., Cavelier, B., Hawes, C., Lerouge, P., and Faye, L., *N*-Glycans harboring the Lewis a epitope are expressed at the surface of plant cells. *Plant J.*, **12**, 1411–1417 (1997).
3) Wilson, I. B. H., Zeleny, R., Kolarich, D., Staudacher, E., Stroop, C. J. M., Kamerling, J. P., and Altman, F., Analysis of Asn-linked glycans from vegetable foodstuffs: widespread occurrence of Lewis a, core α1-3-linked fucose and xylose substitutions. *Glycobiology*, **11**, 261–274 (2001).
4) Alisi, C., Afferni, C., Iacovacci, P., Barletta, B., Tinghino, R., Butteroni, C., Puggioni, E. M. R., Wilson, I. B. H., Federico, R., Schinina, M. E., Ariano, R., Di Felice, G., and Pini, C., Rapid isolation, charcterization, and glycan analysis of Cup a 1, the major allergen of Arizona cypress (*Cupressus arizonica*) pollen. *Allergy*, **56**, 978–984 (2001).
5) Navazio, L., Miuzzo, M., Royle, L., Baldan, B., Varotto, S., Merry, A. H., Harvey, D. J., Dwek, R. A., Rudd, P. M., and Mariani, P., Monitoring endoplasmic reticulumn-to-golgi traffic of a plant carleticulin by protein glycosylation analysis. *Biochemistry*, **41**, 14141–14149 (2002).
6) Hino, K., Yamamoto, S., Sano, O., Taniguchi, Y., Kohno, K., Usui, M., Fukuda, S., Hanzawa, H., Haruyama, H., and Kurimoto, M., Carbohydrate structures of the glycoprotein allergen Cry j 1, from Japanese cedar (*Cryptomeria japonica*) pollen. *J. Biochem.*, **117**, 289–295 (1996).
7) Ogawa, H., Hijikata, A., Amano, M., Kojima, K., Fukushima, H., Ishizuka, I., Kurihara, Y., and Matsumoto, I., Structures and contribution of the antigenicity of oligosaccharides of Japanese cedar (*Cryptomeria japonica*) pollen allergen Cry j I: relationship between the structures of and antigenic epitopes of plant *N*-linked complex-type glycans. *Glycoconjugate. J.*, **13**, 555–566 (1996).
8) Midoro-Horiuti, T., Goldblum, R. M., Kurosky, A., Wood, T. G., Schein, C. H., and Brooks, E. G., Molecular cloning of the mountain cedar (*Juniperus ashei*) pollen major allergen, Jun a 1. *J. Allergy Clin. Immunol.*, **104**, 613–617 (1999).
9) Taniai, M., Ando, S., Usui, M., Kurimoto, M., Sakaguchi, M., Inouye, S., and Matsuhashi, T., *N*-terminal amino acid of major allergen of Japanese cedar pollen (Cry j 1). *FEBS Lett.*, **239**, 329–332 (1988).
10) Kimura, Y., Yoshiie, T., Woo, K. K., Maeda, M., Kimura, M., and Tan, S. H., Structural features of *N*-glycans linked to glycoproteins from oil palm pollen, an allergenic pollen. *Biosci. Biotechnol. Biochem.*, **67**,

2232–2239 (2003).
11) Kimura, Y., Hase, S., Kobayashi, Y., Kyogoku, Y., Ikenaka, T., and Funatsu, G., Structures of sugar chains of ricin D. *J. Biochem.*, **103**, 944–949 (1988).
12) Kimura, Y., Suzuki, M., and Kimura, M., *N*-Linked oligosaccharides of glycoproteins from allergenic *Ginkgo biloba* pollen. *Biosci. Biotechnol. Biochem.*, **65**, 2001–2006 (2001).
13) Natsuka, S., and Hase, S., Analysis of *N*- and *O*-glycans by pyridylamination. *Methods Mol. Biol.*, **76**, 101–113 (1998).
14) Kimura, Y., Ohno, A., and Takagi, S., Structural analysis of *N*-glycans of storage glycoproteins in soybean seeds. *Biosci. Biotechnol. Biochem.*, **61**, 1866–1871 (1997).
15) Sano, M., Hayakawa, K., and Kato, I., An enzyme releasing lacto-*N*-biose from oligosaccharides. *Proc. Natl. Acad. Sci. U.S.A.*, **89**, 8512–8516 (1992).

Available online at www.sciencedirect.com
SCIENCE DIRECT®
European Journal of Pharmacology 524 (2005) 30–37
ELSEVIER
ejp
www.elsevier.com/locate/ejphar

CRTH2-specific binding characteristics of [^{3}H]ramatroban and its effects on PGD_2-, 15-deoxy-$\Delta^{12,14}$-PGJ_2- and indomethacin-induced agonist responses

Hiromi Sugimoto [a,*], Michitaka Shichijo [a,1], Mitsuhiro Okano [b], Kevin B. Bacon [a,2]

[a] *Respiratory Diseases Research, Bayer Yakuhin, Ltd., 6-5-1-3 Kunimidai, Kizu-cho, Soraku-gun, Kyoto 619-0216, Japan*
[b] *Department of Otolaryngology-Head and Neck Surgery, Okayama University Graduate School of Medicine and Dentistry, Japan*

Received 31 March 2005; received in revised form 29 August 2005; accepted 1 September 2005
Available online 27 October 2005

Abstract

We previously showed that ramatroban (Baynas™), a thromboxane A_2 (TxA_2) antagonist, had inhibited prostaglandin D_2 (PGD_2)-stimulated human eosinophil migration mediated through activation of chemoattractant receptor-homologous molecule expressed on Th2 cells (CRTH2). However, detailed pharmacological characterization of its inhibitory activity has not been described. In the present study, we showed that [^{3}H] ramatroban bound to a single receptor site on CRTH2 transfectants with a similar K_d value (7.2 nM) to a TxA_2 receptor (8.7 nM). We also demonstrated that ramatroban inhibited PGD_2-, 15-deoxy-$\Delta^{12,14}$-PGJ_2 (15d-PGJ_2)- and indomethacin-induced calcium responses on CRTH2 transfectants in a competitive manner with similar pA_2 values (8.5, 8.5, and 8.6, respectively). This is the first report showing the evidence for direct binding of ramatroban to CRTH2, revealing its competitive inhibitory effects and another interesting finding that PGD_2, indomethacin and 15d-PGJ_2 share the same binding site with ramatroban on CRTH2.

Keywords: Ramatroban; CRTH2 (Chemoattractant receptor-homologous molecule expressed on Th2 cells); Indomethacin; 15d-PGJ_2 (15-deoxy-$\Delta^{12,14}$-PGJ_2); Competitive inhibitory effect

1. Introduction

Ramatroban (Baynas™, (+)-(3R)-3-(4-fluorobenzensulfonamido)-1,2,3,4-tetra-hydrocarbazole-9-propionic acid), is a potent antagonist of the thromboxane A_2 (TxA_2) receptor (prostanoid TP receptor), and has been used for the treatment of allergic rhinitis in Japan. It was reported that ramatroban antagonizes the contraction of human, guinea-pig, rat and ferret airway smooth muscle induced by the prostanoid TP receptor agonist, 9, 11-dideoxy-9α, 11α-methanoepoxy $PGF_{2\alpha}$ (U-46619) (McKenniff et al., 1991), and prostagrandin D_2 (PGD_2)-mediated human bronchoconstriction (Johnston et al., 1992) via prostanoid TP receptor antagonism (Johnston et al., 1992). However, the lack of evidence for functional prostanoid TP receptor expression on eosinophils (Monneret et al., 2001) suggests that the significant antagonism of eosinophil infiltration into the nasal space and nasal obstruction in allergen-challenged patients suffering from perennial rhinitis by ramatroban (Terada et al., 1998) was not caused solely by prostanoid TP receptor antagonism by ramatroban. We reported that ramatroban inhibited eosinophil migration by interacting with chemoattrantant receptor-homologous molecule expressed on Th2 cells (CRTH2) (Sugimoto et al., 2003). There are, therefore, potentially two mechanisms through which ramatroban can block eosinophil migration into the nasal space. One is that ramatroban inhibits thromboxane-induced adhesion molecule expression on endothelial cells via prostanoid TP receptor antagonism, and another is that ramatroban directly inhibits their migration by CRTH2 antagonism. However, there are no reports describing the comprehensive characterization of

* Corresponding author. Current address: Global Research and Development, Nagoya Laboratories, Pfizer Japan Inc., 5-2 Taketoyo, Aichi, 470-2393, Japan. Tel.: +81 569744867; fax: +81 569744606.
E-mail address: hiromi.sugimoto@pfizer.com (H. Sugimoto).
[1] Current address: Medicinal Biology 2, Discovery Research Laboratories, Shionogi and Co., Ltd., 3-1-1 Futaba-cho, Toyonaka, Osaka, 561-0825, Japan.
[2] Current address: Actimis Pharmaceuticals, Inc., 11099 North Torrey Pines Road, Suite 200, La Jolla, California, 92037, USA.

0014-2999/$ - see front matter © 2005 Elsevier B.V. All rights reserved.
doi:10.1016/j.ejphar.2005.09.005

the interaction of ramatroban with the prostanoid TP receptor and the CRTH2 receptor.

PGD_2, a predominant prostanoid produced by activated mast cells has been implicated in the pathogenesis of allergic asthma and atopic dermatitis (Lewis et al., 1982). PGD_2 is generated by cyclooxygenase (COX)-1 and COX-2 from arachidonic acid and exerts its effects through two G-protein coupled receptors, the PGD_2 receptor (prostanoid DP receptor) (Boie et al., 1995) and CRTH2 (Nagata et al., 1999; Hirai et al., 2001). The prostanoid DP receptor is coupled to G_s-type G proteins (G_s), and increases intracellular cyclic AMP (cAMP) and calcium (Hirata et al., 1994), which mediate both inflammatory and anti-inflammatory events (Matsuoka et al., 2000), and inhibition of colonic granulocyte infiltration in the rat (Ajuebor et al., 2000). CRTH2 is coupled to G_i-type G proteins (G_i), and inhibits cAMP production and increases intracellular calcium (Hirai et al., 2001), which mediate pro-inflammatory effects including migration or degranulation of eosinophils (Hirai et al., 2001; Gervais et al., 2001). It is also known that PGD_2 induces the contraction of human isolated bronchial smooth muscle via a prostanoid TP receptor (Coleman and Sheldrick, 1998). The prostanoid TP receptor couples to G_q-type G proteins (G_q), activates phospholipase C (PLC) and subsequently increases inositol triphosphate (IP_3), diacylglycerol (DAG) and intracellular calcium concentrations (Hirata et al., 1991). Thus, PGD_2 induces both inflammatory and anti-inflammatory effects via three different G-protein coupled receptors; prostanoid DP receptors, CRTH2 and prostanoid TP receptors.

Recently, it was described that 15-deoxy $\Delta^{12,14}$-PGJ_2 (15d-PGJ_2), a metabolite of PGD_2, and indomethacin bound to CRTH2 and induced migration or degranulation of eosinophils (Hirai et al., 2002; Monneret et al., 2002). 15d-PGJ_2 is known as an agonist of the peroxisome proliferator-activated receptor (PPAR)γ (Forman et al., 1995), which plays a central role in the adipogenesis, enhances the sensitivity to insulin, and inhibits inflammatory responses (Murphy and Holder, 2000).

In the present study, we showed, using human CRTH2 transfectants, that ramatroban bound to CRTH2 with high affinity comparable to the prostanoid TP receptor, and that ramatroban antagonized CRTH2 in a competitive manner. Furthermore, we examined the effects of ramatroban on CRTH2 activities induced by 15d-PGJ_2 and indomethacin, also recently identified as CRTH2 agonists.

2. Materials and methods

2.1. Reagents

Ramatroban was synthesized at Bayer Yakuhin Ltd. (Shiga, Japan).[^{3}H]ramatroban and (*E*)-5-[[[(3-pyridinyl)[3-(trifluoromethyl)phenyl]-methylen]amino]oxy] pentanoic acid (ridogrel) were prepared at Bayer AG. (Wuppertal, Germany). PGD_2 was purchased from Sigma-Aldrich (St. Louis, MO). 13, 14-dihydro-15-keto-prostaglandin D_2 (13, 14-dihydro-15-keto-PGD_2), 15R-methyl-prostaglandin D_2 (15R-methyl-PGD_2), 15-Deoxy-$\Delta^{12,14}$-prostaglandin J_2 (15d-PGJ_2), 7-[3-[[2-[(phenylamino)carbonyl] hydrazino]methyl]7-oxabicyclo[2.2.1]hept-2-yl]-,[1*S*-[1α, 2α(*Z*), 3α, 4α]]-]5-heptenoic acid (SQ29548) and 5-(6-Carboxyhexyl)-1-(3-cyclohexyl-3-hydroxypropyl) hydantoin (BW245C) were purchased from Cayman (Ann Arbor, MI). 9, 11-dideoxy-9α, 11α-methanoepoxy $PGF_{2\alpha}$ (U46619) and 3-isobutyl-1-methylxanthin (IBMX) were purchased from BIOMOL Research Labs Inc. (Plymouth Meeting, PA). Fluo-3AM and pluronic F-127 were purchased from Molecular Probes (Eugene, OR).

2.2. Generation of human CRTH2 transfectants

The human CRTH2 stable transfectants were generated as described previously (Sugimoto et. al., 2003). Briefly, the pEAK10 expression vector containing human *CRTH2* gene was transfected into L1.2 cells (a kind gift from Prof. Eugene Butcher, Stanford, CA) by electroporation (250V/1000 μF; Gene Pulser II, Bio-Rad, Hercules, CA). Stable transfectants were selected in the presence of puromycin (1 μg/ml, P7255, Sigma-Aldrich) and maintained in RPMI-1640 medium (Gibco BRL, Scotland, U.K.) supplemented with 10% heat-inactivated fetal calf serum (JRH Biosciences, KS), 292 μg/ml L-glutamine, 100 IU/ml penicillin, and 100 μg/ml streptomycin (Invitrogen, St. Louis, MO).

In preliminary experiments, the concentrations of dimethyl sulfoxide (DMSO) in working dilutions used in this study (<0.1%) were shown to have no effect on receptor binding, Ca^{2+} mobilization, cAMP production and cell migration assays. We also confirmed that there were no functional prostanoid DP or TP receptors on CRTH2-transfected L1.2 cells (Sugimoto et al., 2003).

2.3. Receptor binding assay

CRTH2 transfectants were suspended in binding buffer (50 mM Tris-HCl, pH 7.4, 40 mM $MgCl_2$, 0.1% bovine serum albumin, 0.1% NaN_3). Cell suspension (2×10^5 cells) and [^{3}H] ramatroban were mixed in a 96-well U-bottom polypropylene plate and incubated for 60 min at room temperature. After incubation, the cell suspension was transferred to a filtration plate (#MAFB, Millipore, Bedford, MA) and washed 3 times with binding buffer. Scintillant was added to the filtration plate, and radioactivity remaining on the filter was measured by a scintillation counter, TopCount (Packard Bioscience, Meriden, CT). For saturation binding experiments, non-specific binding was determined by incubating the cell suspension in the presence of 100 μM unlabeled ramatroban. Competitive binding experiments were performed in the presence of 2.5 nM [^{3}H]ramatroban and various concentrations of competitive ligands.

2.4. Ca^{2+} mobilization assay

Ca^{2+} loading buffer was prepared by mixing 1 μM of Fluo-3AM and pluronic F-127 in Ca^{2+} assay buffer (20 mM HEPES, pH 7.6, 0.1% bovine serum albumin, 1 mM probenecid, Hanks' solution). The CRTH2 transfectants were suspended in Ca^{2+}

loading buffer at 6×10^6 cells/ml, and incubated for 60 min at room temperature. After the incubation, cells were washed and resuspended in Ca^{2+} assay buffer, then dispensed into transparent-bottom 96-well plates (#3631, Costar, NY) at 2×10^5 cells/well. Cells were incubated with various concentrations of ramatroban for 5 min at room temperature. Fluorescence was measured with emission at 480 nm on a FDSS6000 fluorometer (Hamamatsu Photonics, Hamamatsu, Japan).

2.5. cAMP production assay

CRTH2 transfectants were suspended in cAMP assay buffer (20 mM HEPES, pH 7.4, 0.1% bovine serum albumin, 250 mM IBMX, Hanks' solution) at 5×10^5 cells/well and incubated with various concentrations of ramatroban for 5 min at room temperature. After stimulation with 10 μM of forskolin for 5 min, cells were incubated with various ligands for 30 min at 37 °C, 5% CO_2. The cAMP content was determined using cAMP-Screen™ System (Applied Biosysytems, Foster City, CA). Maximal inhibition of forskolin-stimulated cAMP production was determined in the presence of 1 μM PGD_2. In preliminary experiments, the production of cAMP was not observed after pre-incubation with ramatroban alone.

2.6. Migration assay

CRTH2 transfectants were suspended in migration buffer (20 mM HEPES, pH 7.6, 0.1% bovine serum albumin, Hanks' solution) at 4×10^6 cells/ml. Fifty micro liters of the cell suspension (2×10^5 cells/well) was then dispensed into the upper chamber and 30 μl of ligand solution was added to the lower chamber of a 96-well type migration chamber (diameter=5 μm, #106-5, Neuro Probe, Gaithesburg, MD). Cells were pre-incubated with various concentrations of ramatroban for 10 min at 37 °C. The migration assay was performed in a humidified incubator at 37 °C, 5% CO_2 for 4 h. The number of cells migrated into the lower chamber was counted by a fluorescence activated cell sorter (FACS), as described previously (Palframan et al., 1998).

3. Results

3.1. Binding profile of [^{3}H]ramatroban to CRTH2

Receptor binding assays were performed to investigate the binding profile of [^{3}H]ramatroban to CRTH2. [^{3}H]ramatroban bound to CRTH2 transfectants in a concentration-dependent and saturable manner but not to non-transfected parental cells (Fig. 1A). From a Scatchard plot analysis, the K_d and B_{max} values were calculated as 7.2 nM and 92.5 pM (a number of 27,800 binding sites/transfectant), respectively (Fig. 1B). Hill plot analysis showed a slope of 1.00, signifying a non-cooperative bimolecular interaction between ramatroban and CRTH2 (Fig. 1C). In competitive binding assays, non-labeled ramatroban inhibited the binding of [^{3}H]ramatroban to CRTH2 in a concentration-dependent manner with a K_i value of 41 nM (Fig. 2B). The binding of [^{3}H]ramatroban to CRTH2 was inhibited by CRTH2 agonists such as PGD_2, 13, 14-dihydro-15-keto-PGD_2 or 15R-methyl-PGD_2 with K_i values of 23, 40, and 1.2 nM, respectively, but not by the prostanoid TP receptor agonist, U46619, or prostanoid DP receptor agonist, BW245C, up to 10 μM (Fig. 2A). Indomethacin also inhibited the binding of [^{3}H]ramatroban to CRTH2 in a concentration-dependent manner with a K_i value of 890 nM, which was 20-fold lower affinity than that of ramatroban (Fig. 2B). Prostanoid TP receptor antagonists, SQ29548 and ridogrel did not show any effects up to 10 μM (Fig. 2B).

3.2. Effects of ramatroban on various CRTH2 agonists-induced Ca^{2+} mobilization in CRTH2 transfectants

At first, we confirmed that neither PGD_2 nor U46619 induced Ca^{2+} mobilization in empty vector-transfected or in non-transfected parental cells. This suggests that there are no functional CRTH2, prostanoid DP or TP receptors on parental cells. We also confirmed that U46619 did not induce Ca^{2+} mobilization in CRTH2-transfectants and BWA868C did not inhibit PGD_2-induced Ca^{2+} mobilization in CRTH2 transfectants. These results suggest that there are no functional prostanoid TP or DP receptors on CRTH2-transfectants. Then,

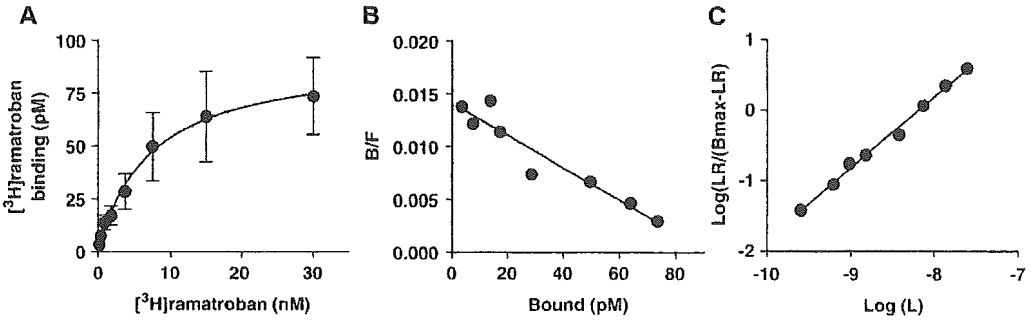

Fig. 1. The binding of [^{3}H]ramatroban to CRTH2 transfectants. (A) Saturation binding of [^{3}H]ramatroban to CRTH2 transfectants. (B) Scatchard plot of [^{3}H] ramatroban binding to CRTH2 transfectants. (C) Hill plot of [^{3}H]ramatroban binding to CRTH2 transfectants. Various concentrations of [^{3}H]ramatroban were incubated with CRTH2 transfectants as described in the Methods. Non specific binding was obtained by incubating with 100 μM unlabeled ramatroban. Data represent mean values±S.E.M. of 5 independent experiments.

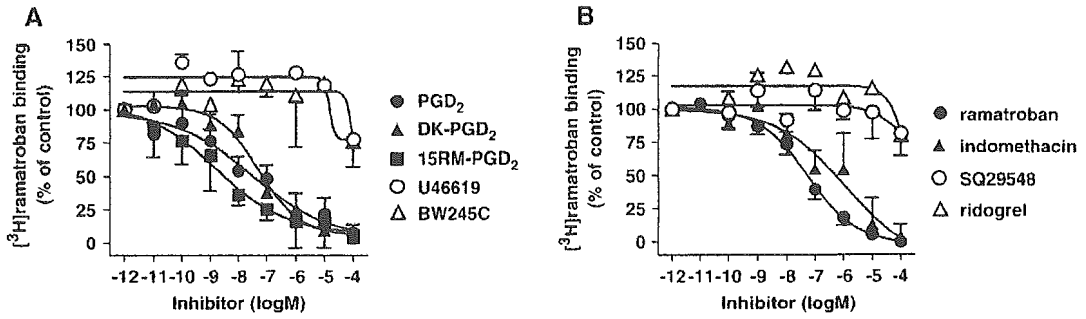

Fig. 2. Effects of ramatroban on [3H]ramatroban binding to CRTH2 transfectants. (A) CRTH2 transfectants were incubated with 2.5 nM [^{3}H]ramatroban together with various agonists such as PGD_2 (n=5), 13, 14-dihydro-15-keto-PGD_2 (DK-PGD_2, n=9), 15R-methyl-PGD_2 (15RM-PGD_2, n=3), U46619 (n=4) or BW245C (n=4). (B) CRTH2 transfectants were incubated with 2.5 nM [^{3}H]ramatroban together with various antagonists such as ramatroban (n=9), indomethacin (n=3), SQ29548 (n=5) or ridogrel (n=2). Data represent mean values±S.E.M.

we evaluated the effects of various CRTH2 agonists on CRTH2 by using CRTH2-transfectants.

Various CRTH2 agonists, such as PGD_2, 13, 14-dihydro-15-keto-PGD_2 and 15R-methyl-PGD_2, induced Ca^{2+} mobilization in CRTH2 transfectants with EC_{50} values of 1.2, 3.1, and 1.6 nM, respectively (Fig. 3A). These agonist-induced Ca^{2+} responses were inhibited by ramatroban in a concentration-dependent manner with IC_{50} values of 160, 110, and 760 nM, respectively (Fig. 3B).

The PPARγ agonist, 15d-PGJ_2 and a COX inhibitor, indomethacin also induced Ca^{2+} responses in CRTH2 transfectants and this was confirmed in our study with EC_{50} values of 110 and 49 nM, respectively (Fig. 3A). However, 15d-PGJ_2 induced a greater Ca^{2+} response at higher concentrations compared to other CRTH2 agonists (Fig. 3A). Ramatroban inhibited 15d-PGJ_2- and indomethacin-induced Ca^{2+} mobilization in a concentration-dependent manner with IC_{50} values of 46 and 37 nM, respectively (Fig. 3B).

3.3. Competitive inhibitory effects of ramatroban on CRTH2 activation

To further examine the inhibitory effects of ramatroban on CRTH2 activation, we performed PGD_2-induced Ca^{2+} mobilization assays in CRTH2 transfectants in the presence of various concentrations of ramatroban. Ramatroban caused a concentration-related rightward shift of the PGD_2 concentration–response curves with a pA_2 value of 8.5 and slope value of 0.81 as assessed by Schild plot (Fig. 4A), suggesting that ramatroban is a competitive antagonist for human CRTH2. Ramatroban also shifted the concentration–response curves of 13, 14-dihydro-15-keto-PGD_2 and 15R-methyl-PGD_2 to the right with pA_2 values of 8.1 and 7.8, with slope values of 0.81 and 0.83, respectively (data not shown). Furthermore, ramatroban caused a concentration-related rightward shift of the 15d-PGJ_2 and indomethacin concentration–effect curves with pA_2 values of 8.5 and 8.6, and slope values of 0.81 or 0.76, respectively (Fig. 4B, C).

3.4. Effects of ramatroban on cAMP production stimulated by indomethacin and 15d-PGJ_2 in human CRTH2 transfectants

Another functional assay, cAMP production, was measured to investigate the effects of ramatroban on 15d-PGJ_2-or indomethacin-treated CRTH2 transfectants. Various CRTH2 agonists such as PGD_2, 13, 14-dihydro-15-keto-PGD_2 and 15R-methyl-PGD_2 reduced forskolin-induced cAMP production in CRTH2 transfectants with EC_{50} values of 0.24, 2.8, and 0.43 nM, respectively (Fig. 5A). These effects by PGD_2, 13, 14-dihydro-15-keto-PGD_2 and 15R-methyl-PGD_2 were reversed by ramatroban in a concentration-dependent manner (Fig. 5B). 15d-PGJ_2 and indomethacin also reduced

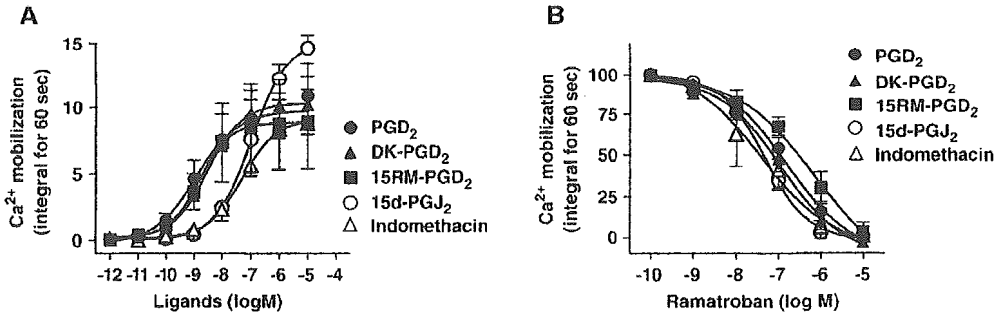

Fig. 3. Effects of ramatroban on Ca^{2+} mobilization in CRTH2 transfectants. (A) Concentration-response of Ca^{2+} mobilization in CRTH2 transfectants induced by PGD_2 (n=4), 13, 14-dihydro-15-keto-PGD_2 (DK-PGD_2, n=4), 15R-methyl-PGD_2 (15RM-PGD_2, n=3), 15d-PGJ_2 (n=3) or indomethacin (n=3). (B) Effects of ramatroban on Ca^{2+} mobilization in CRTH2 transfectants induced by 10 nM PGD_2 (n=4), 13, 14-dihydro-15-keto-PGD_2 (DK-PGD_2, n=4), 15R-methyl-PGD_2 (15RM-PGD_2, n=3) or 100 nM 15d-PGJ_2 (n=3), indomethacin (n=3). Data represent mean values±S.E.M.

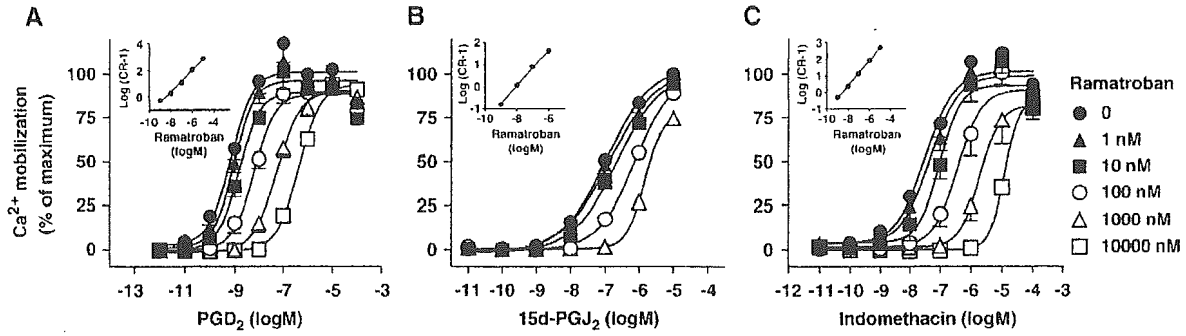

Fig. 4. Competitive inhibitory effects of ramatroban on CRTH2. CRTH2 transfectants were incubated with various concentrations of ramatroban and Ca^{2+} mobilization induced by various concentrations of PGD_2 (A. $n=4$), 13, 14-dihydro-15-keto-PGD_2 (DK-PGD_2, $n=4$), 15R-methyl-PGD_2 (15RM-PGD_2, $n=3$), 15d-PGJ_2 (B. $n=3$) or indomethacin (C. $n=3$) were monitored. pA_2 values were calculated by Schild plots.

forskolin-induced cAMP production in CRTH2 transfectants with EC_{50} values of 49 and 4.5 nM, respectively (Fig. 5A). These effects by 15d-PGJ_2 and indomethacin were reversed by ramatroban in a concentration-dependent manner (Fig. 5B).

3.5. Effects of ramatroban on indomethacin- and 15d-PGJ_2-mediated migration of CRTH2 transfectants

It is well known that cells such as eosinophils expressing CRTH2 migrate in response to PGD_2. We investigated the effects of ramatroban on CRTH2 ligand-induced migration using human CRTH2 transfectants. PGD_2, 14-dihydro-15-keto-PGD_2 and 15R-methyl-PGD_2-stimulated transfectants demonstrated characteristic bell-shaped concentration-dependent migration responses. The half maximal responses (EC_{50} values) were achieved at 0.5, 1.3, and 0.2 nM, respectively (Fig. 6A). 15R-methyl-PGD_2 produced three-fold greater response in the number of cells migrated when compared with PGD_2 and 14-dihydro-15-keto-PGD_2. Ramatroban completely blocked the migration of CRTH2 transfectants induced by sub-optimal concentrations of PGD_2 (1 nM), 14-dihydro-15-keto-PGD_2 (3 nM), or 15R-methyl-PGD_2 (1 nM), in a concentration-dependent manner with IC_{50} values of 140, 140, or 43 nM, respectively (Fig. 6C). Indomethacin and 15d-PGJ_2 similarly demonstrated bell-shaped dose–response curves in migration assays. Compared with 15R-methyl-PGD_2, both indomethacin and 15d-PGJ_2 were less potent, with EC_{50} values of 40 and 32 nM, respectively (Fig. 6B). The maximal response of indomethacin was similar to that of 15R-methyl-PGD_2 but the response of 15d-PGJ_2 was far greater than that of 15R-methyl-PGD_2. Ramatroban completely blocked the migration of CRTH2 transfectants induced by sub-optimal concentrations of indomethacin (100 nM) and 15d-PGJ_2 (100 nM) in a concentration-dependent manner with IC_{50} values of 120 and 60 nM, respectively (Fig. 6D).

4. Discussion

In this report, we showed that [^{3}H]ramatroban bound to CRTH2 with a K_d value of 7.2 nM (Fig. 1). We also demonstrated that ramatroban caused a concentration-related rightward shift of the PGD_2 concentration–response curves with a pA_2 value of 8.5 in the PGD_2-induced Ca^{2+}mobilization assay (Fig. 4A). The K_d value of [^{3}H]ramatroban binding to the prostanoid TP receptor on human platelets was reported as 8.7 nM (Theis et al., 1992) and the pA_2 value for ramatroban antogonism of U46619 (prostanoid TP receptor agonist)-induced contractions of human pulmonary vein smooth muscle was reported as 8.9 (Walch et al., 2001). These results suggest that ramatroban bound to CRTH2 and the prostanoid TP

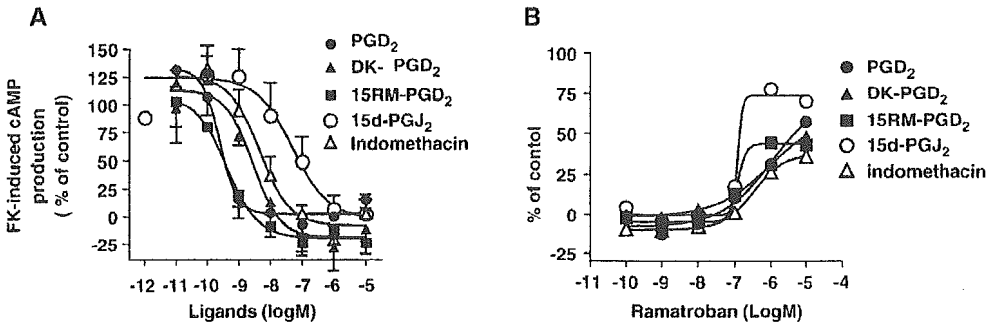

Fig. 5. Effects of ramatroban on cAMP production in CRTH2 transfectants. (A) Concentration-response of 10 μM forskolin (FK)-induced cAMP production in CRTH2 transfectants induced by PGD_2 ($n=6$), 13, 14-dihydro-15-keto-PGD_2 (DK-PGD_2, $n=4$), 15R-methyl-PGD_2 (15RM-PGD_2, $n=4$), 15d-PGJ_2 ($n=6$) or indomethacin ($n=6$). Data represent mean values±S.E.M. (B) Effects of ramatroban on 10 μM forskolin (FK)-induced cAMP production in CRTH2 transfectants induced by 10 nM PGD_2 ($n=2$), 100 nM 13, 14-dihydro-15-keto-PGD_2 (DK-PGD_2, $n=2$), 10 nM 15R-methyl-PGD_2 (15RM-PGD_2, $n=2$), 1000 nM 15d-PGJ_2 ($n=2$) or 100 nM indomethacin ($n=2$).

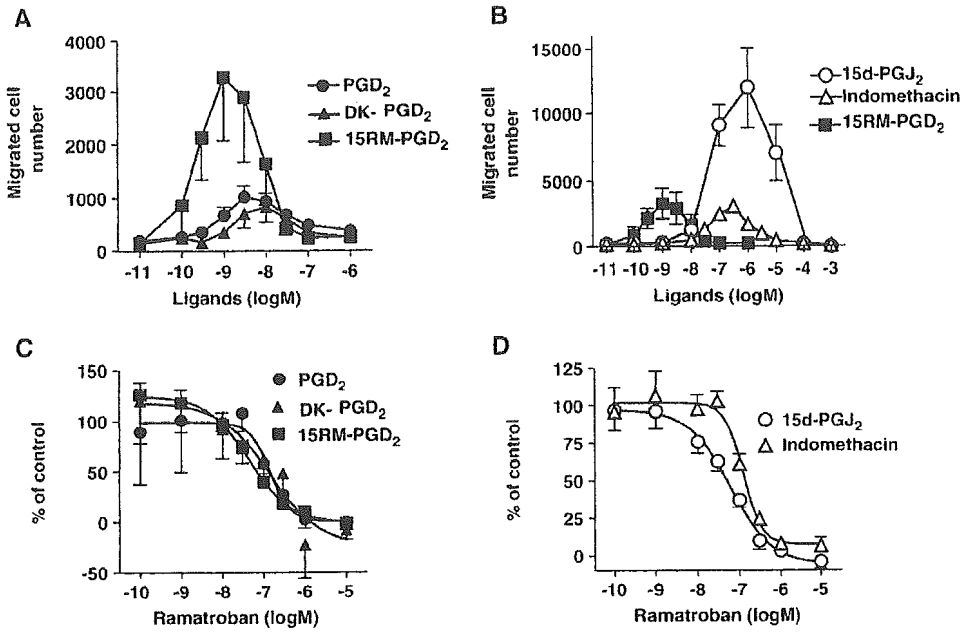

Fig. 6. Effects of ramatroban on migration of CRTH2 transfectants. (A, B) Concentration-response of migration of CRTH2 transfectants induced by PGD_2 (n=5), 13, 14-dihydro-15-keto-PGD_2 (DK-PGD_2, n=4), 15R-methyl-PGD_2 (15RM-PGD_2, n=3), 15d-PGJ_2 (n=5) or indomethacin (n=4). (C, D) Effects of ramatroban on migration of CRTH2 transfectants induced by 1 nM PGD_2 (n=7), 3 nM 13, 14-dihydro-15-keto-PGD_2 (DK-PGD_2, n=3), 1 nM 15R-methyl-PGD_2 (15RM-PGD_2, n=4), 100 nM 15d-PGJ_2 (n=4) or 100 nM indomethacin (n=4). Data represent mean values±S.E.M.

receptor with a similar affinity and its inhibitory effects on CRTH2 and the prostanoid TP receptor are competitive in manner. These findings will be critical reference points in experimental settings using ramatroban as a research tool, and in the clinical setting. These results also strongly support our previous report (Sugimoto et al., 2003). In our previous report, we showed that ramatroban, which had been thought of as a specific prostanoid TP receptor antagonist, antagonized CRTH2 activities with IC_{50} values of 100, 30 and 170 nM in [^{3}H]PGD_2 binding to CRTH2, PGD_2-induced Ca^{2+}mobilization in CRTH2 transfectants and PGD_2-induced migration of human eosinophils, respectively. Based on these results, we suggested that ramatroban antagonizes eosinophil recruitment into tissue by at least two different mechanisms; via the prostanoid TP receptor and CRTH2. Through prostanoid TP receptor antagonism on endothelial cells, ramatroban inhibits eosinophil adhesion to endothelial cells by inhibiting the TxA_2-mediated expression of intercellular adhesion molecule-1 (ICAM-1) and vascular cell adhesion molecule-1 (VCAM-1) on human vascular endothelial cells (Ishizuka et al., 1998, our unpublished data). Through CRTH2 antagonism, ramatroban inhibits migration of eosinophils directly.

Our present study reveals another interesting results using indomethacin. Indomethacin is known as an anti-inflammatory agent for its inhibitory effects on COXs and recently it was reported that indomethacin was also an activator of CRTH2. In our experiment, indomethacin completely inhibited the binding of [^{3}H]ramatroban to CRTH2, although the affinity was 20-fold weaker (K_i=890 nM) than that of ramatroban (K_i=41 nM) (Fig. 2). We further studied the signaling mechanism of indomethacin and ramatroban through CRTH2 to clarify these mechanisms. Indomethacin induced Ca^{2+} mobilization in CRTH2 transfectants with the same efficacy as PGD_2 and other CRTH2 ligands such as 13, 14-dihydro-15-keto-PGD_2 or 15R-methyl-PGD_2, although the potency was 30 to 40-fold weaker than those of CRTH2 ligands. Ramatroban inhibited indomethacin-induced Ca^{2+} mobilization completely and caused a concentration-related rightward shift of the indomethacin concentration–response. These results suggest that ramatroban inhibits indomethacin-induced Ca^{2+} mobilization in a competitive inhibitory manner, suggesting that indomethacin shares the same binding site with ramatroban on CRTH2.

15d-PGJ_2 is known to have anti-inflammatory actions based on its agonistic effects on PPARγ and it was reported recently that 15d-PGJ_2 was also an activator for CRTH2. Interestingly, 15d-PGJ_2 induced Ca^{2+} mobilization in CRTH2 transfectants with greater efficacy than those of other CRTH2 ligands. This response was inhibited completely by ramatroban, suggesting that it was mediated via CRTH2. Furthermore, ramatroban also caused a concentration-related rightward shift of the 15d-PGJ_2 concentration–response curves. This result suggests that ramatorban inhibits 15d-PGJ_2-induced Ca^{2+} mobilization in a competitive manner, suggesting that 15d-PGJ_2 also shares a similar binding site with ramatroban on CRTH2.

Furthermore, indomethacin and 15d-PGJ_2 reduced forskolin-induced cAMP production, and induced cell migration of CRTH2 transfectants. Ramatroban inhibited all of these responses. Thus, ramatroban demonstrated antagonistic effects on responses induced by indomethacin and 15d-PGJ_2 via CRTH2, which further compounds the mechanisms by which they exert their anti-inflammatory action—through inhibition of COXs or activation of PPARγ. While this is counterintuitive it may be one